Draft version September 2, 2021
Typeset using LaTeX **twocolumn** style in AASTeX63

Modeling the Ionized Gas in the Central Starburst Region of M82

Kara N. Green[1] and Kimberly L. Emig[2]

[1] *West Virginia University,*
[2] *National Radio Astronomy Observatory,*

(Received ...; Revised ...; Accepted ...)

Submitted to NRAO REU 2021

ABSTRACT

This report presents a model of the ionized gas of the central starburst region of M82, a nearby starburst galaxy of a distance (3.6 Mpc), from measurements of the radio recombination line emission of hydrogen. We obtained 8 measurements of the hydrogen radio recombination line emission with frequencies ranging from 1.425 GHz to 316 GHz. A best fit line with a slope of ∼1.0723 was plotted to the higher frequency data points and analyzed to further investigate the composition of the center region of ionized gas. Geometrical assumptions of the interstellar medium were formed to derive a pathlength, density, and emission measure of the region and produce models of the radio recombination line emission. We find one model that outlines the general behavior of the measurements. The next steps of this project will be to determine a goodness of fit and include HII regions and synchrotron radiation at the lower frequencies to understand the ISM of the central starburst region of M82.

Keywords: galaxies: individual (M82) – galaxies: ISM – galaxies: starburst – galaxies: star clusters: general – galaxies: star formation

1. INTRODUCTION

Figure 1. Optical image of starburst galaxy M82.

Corresponding author: Kara N.Green
kng0018@mix.wvu.edu

Many stars form in compact massive star clusters where a high density of gas is produced at high temperatures. This creates an environment of high star formation rate and contributes to the evolution of the host galaxy. Starburst galaxies consist of extremely high star forming regions where most of the high-density gas is compact at the center region of the galaxy. The structure of the interstellar medium (ISM) and the relationship between the ionized gas and star formation rates differentiate starburst galaxies from other systems.

M82 is a nearby starburst galaxy at a distance 3.6 Mpc. M82 contains a center region of warm ionized gas of about 1 kpc in size and interacts with a neighboring galaxy, M81 (Rodriguez-Rico et al. 2004). This interaction triggers a production of high star forming regions within M82 at a rate of 10 $M_\odot$ yr^{-1}, which is about 33 times greater than that of the Milky Way (Rodriguez-Rico et al. 2004). In this center region, massive star clusters create compact regions that contain ionized hy-

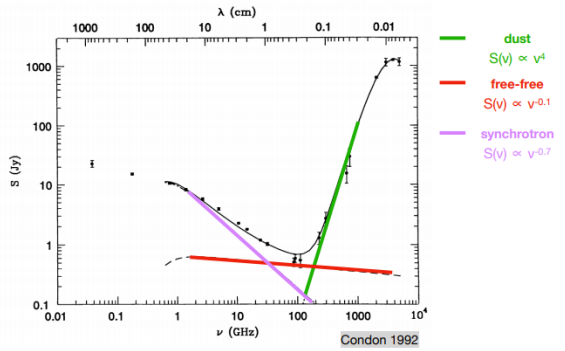

Figure 2. Integrated radio continuum measurements for entire starburst galaxy M82.

drogen gas at temperatures of about 10,000 Kelvin with densities greater than 1,000 cm^{-3}.

These compact regions of ionized hydrogen gas are called HII regions, which outline the star formation of the galaxy and emit free-free continuum radiation. As a free electron passes by a free proton, the interaction between the two produces emission known as free-free continuum radiation. Free-free continuum radiation is mostly observed in HII regions due to the high energy and photoionization of the gas from the massive star clusters.

In this report, we focus on the central starburst region of M82 at a frequency range of about 1 GHz to 300 GHz. In Figure 2, the total radio continuum flux density of the galaxy, M82, is displayed and classified according to wavelength. Free-free continuum radiation is present throughout the galaxy. However, at the lower frequencies and longer wavelengths ($\gtrsim$ 40 GHz) synchrotron radiation dominates the continuum emission. At higher frequencies and shorter wavelengths, dust is mostly observed in the galaxy. In the central starburst region of M82, free-free continuum emission dominates the radiation observed in the central starburst region.

2. DATA

We compiled 8 hydrogen radio recombination line measurements of M82 from different papers (Seaquist et al. 1996; Puxley et al. 1989; Shaver et al. 1977; Bell & Seaquist 1977; Bell et al. 1984; Chaisson & Rodriguez 1977; Seaquist et al. 1994, 1985) observed from a variety of radio telescopes including the Very Large Array, James Clark Maxwell Telescope, and the Millimeter Array of the Owens Valley Radio Observatory. Table 1 identifies the hydrogen line with the quantum number, the integrated recombination line flux density at different epochs, angular resolution, FWHM linewidth sizes of 149–338 km/s, and the telescope that was used for each measurement. Observations of these measurements were taken at frequencies ranging from 1.425 GHz to 316.4156 GHz with angular resolutions between 4 arcseconds and 10 arcminutes. The integrated recombination line flux density (mJy km/s) of the measurements is plotted to frequency (GHz) as seen in Figure 2.

$$S = 65.13\times\left(\frac{EM}{5\times10^{8}}\right)\left(\frac{D}{3.8pc}\right)^{-2}\left(\frac{T_e}{10^{4}K}\right)^{-1.5}\left(\frac{\nu}{100GHz}\right) \quad (1)$$

To model these frequency points we used Equation 1 to calculate the emission measure for the H27α line. In Equation 1, the integrated flux density is represented as S, the emission measure of the region is EM, the distance is shown as D, the temperature is represented as T_e, and the observed frequency is ν. Table 1 shows the hydrogen alpha lines, the integrated flux density, the frequency of the measurements, the angular resolution, the linewidth, and the telescope used. From Table 1, we utilized the integrated flux density, S, a distance $D = 3.6$ Mpc, a temperature $T = 10000$ K, and the observed frequency ν for the H27α measurement. We computed an emission measure of $\sim$3.55x10^{11} from Equation 1 with these values. This condition allowed us to find the slope that outlines the 4 high frequency measurements to model the behavior of the recombination line emission. Using the calculated emission measure, the array of frequencies and the integrated flux densities of all 8 hydrogen lines, we computed a slope of $\sim$1.0723. Through analyzing Equation 1, we determined the expected value of the slope to be 1. Comparing this with the calculated value, we implemented the expected slope into the model to plot a best fit line to the high frequency data points shown in Figure 3: H27α, H30α, H41α, and H53α.

3. RESULTS

The best fit line plotted to the measurements only outlines the high frequency points. To model the low frequency data points as well, an assumption of the composition and shape of the center region of M82 is formulated. Here, we assume that the recombination line emission is mostly produced by diffused ionized gas. Figure 4 shows the 92 GHz integrated radio flux density continuum distribution of M82 from (Seaquist et al. 1996) with a cylindrical outline of the center region. It is assumed that the diffused gas is dispersed throughout the entirety of this cylindrical region. Through geometric assumptions, we derived a pathlength of $\sim$1.29 x 10^3

Table 1. Radio Recombination Line Measurements From M82

Hydrogen Line	Integrated Flux Density	Frequency	Angular Resolution	Linewidth	Telescope	References[a]
...	W/m^2	GHz	as	km/s	...	
H27α	21.1 ± 4.3	316.4156	15.2	...	James Clark Maxwell Telescope (JCMT)	1
H30α	5.12 ± 1.0	231.9009	21	...	JCMT	2
H41α	1.32 ± 0.22	92.0344	4.5	...	OVRA Millimeter Array	1
H53α	0.22 ± 0.06	42.952	41	...	Nobeyama Radio Observatory	3
H85α	$(4.6 \pm 0.7) \times 10^{-3}$	10.522	$2.8(am)$	149 ± 25	Alonquin Radio Observatory	4
H102α	$8.5 \pm 1.4e-3$	6.107	$4(am)$	174 ± 28	Alonquin Radio Observatory	4
H110α	$1.05 \pm 0.1e-2$	4.874	5.7	293 ± 20	Westerbrook Synthesis Radio Telescope	5
H167α	$5.1 \pm 0.8e-3$	1.425	17	338 ± 40	Westerbrook Synthesis Radio Telescope	5

NOTE—The integrated flux density is measured over the central starburst region of M82 at different frequencies (seen in column 3).
[a] References: (1) Seaquist et al. (1996), (2) Seaquist et al. (1994), (3) Puxley et al. (1989), (4) Bell & Seaquist (1977), (5) Shaver et al. (1977)

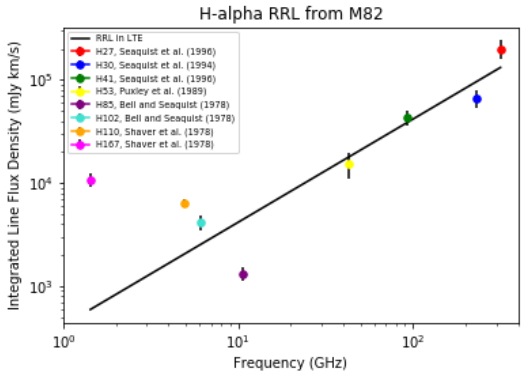

Figure 3. Integrated hydrogen radio recombination line flux density of center region for 8 frequencies. A best fit line with a slope of ~1.0723 is tracing the 4 high frequency data points

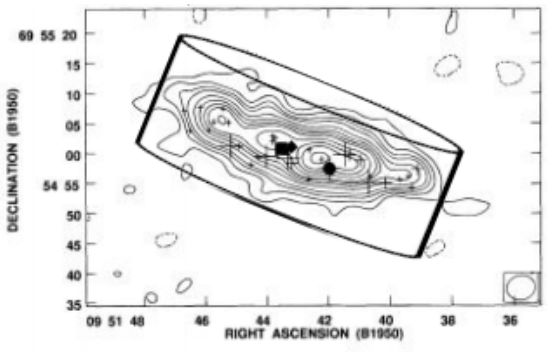

Figure 4. 92 GHz integrated radio flux density continuum distribution of M82 with cylindrical estimate of region outline.

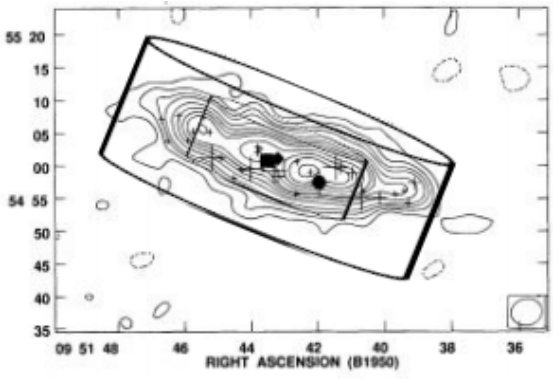

Figure 5. 92 GHz integrated radio flux density continuum distribution of M82 with ring or donut-shaped outline.

pc and a density of ~30 cm^{-3} for this region. Figure 5 shows the 92 GHz integrated radio flux density continuum distribution of M82 from (Seaquist et al. 1996) with a ring or donut-shaped outline of the center region. It is assumed that the diffused gas is more condensed in the outer ring of the center region. Through geometrical assumptions, a pathlength of ~4.47 x 10^2 pc and a density of ~50 cm^{-3} was derived.

$$S_l = \frac{2k\nu^2}{c^2}\Omega_l T_e \left[\frac{b_m \tau_c}{\tau_l + \tau_c}\left(1 - e^{-\tau_l+\tau_c}\right) - \left(1 - e^{-\tau_c}\right)\right] + S_{cbg} e^{-\tau_c}\left(e^{-\tau_l} - 1\right) \quad (2)$$

From these assumptions, we used Equation 2 to create models for the recombination line measurements of the peak flux density. In Equation 2, S_l is the total internal line emission and stimulated emission of the region, Ω_l is the observed solid angle of the region, S_{cbg} is the background non-thermal continuum emission, k is the Boltzmann constant, τ_c is the continuum optical depth, τ_l is the peak line optical depth and τ_s is the peak line optical depth under LTE conditions. This equation is

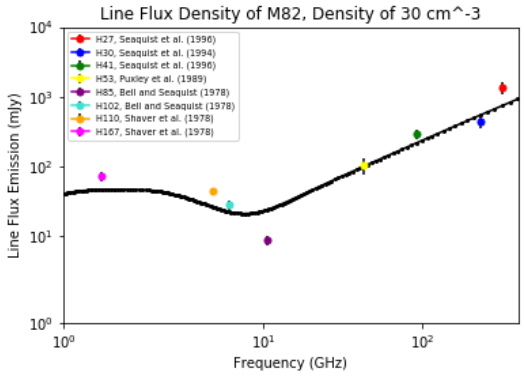

Figure 6. Model of peak flux density predicted for estimated cylinder shaped region of density 30 cm^{-3}. Peak line emission vs. frequency is plotted. The black line represents the model. The colored data points represent the measurements of the recombination line emission.

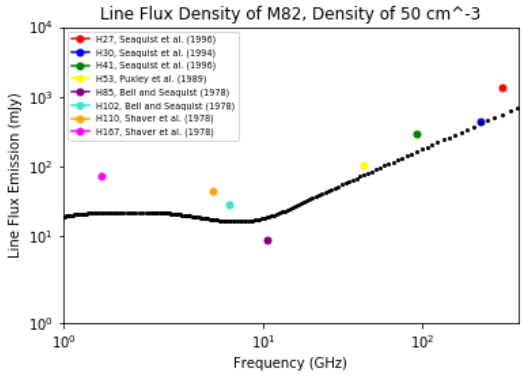

Figure 7. Model of peak flux density predicted for estimated cylinder shaped region of density 50 cm^{-3}. Peak line emission vs. frequency is plotted. The black line represents the model. The colored data points represent the measurements of the recombination line emission.

used to calculate the modeled recombination line emission from the center region of M82. Using the quantities obtained in our assumptions, we produced models for the assumed cylinder-shaped region (Figure 6) and the ring-shaped region (Figure 7).

4. DISCUSSION

For the Figure 6 and Figure 7, the peak line emission at different frequencies is plotted. In Figure 6, the model outlines the recombination line measurements and follows the general behavior of the points. This shows that there is a possibility of diffused ionized gas at the lower frequencies. However, this black line for this assumed cylindrical region is imprecise. Likewise, for Figure 7, the black line, which represents the model, is imprecise nor does it follow the general behavior for the measurements. In Figure 7, our assumed geometry was a ring with a derived density of $\sim$50 cm^{-3}. The impreciseness of Figure 7 could be a result of our miscalculations for the density. To correct this inaccuracy, the density for the assumed ring region would need to increase to better fit the recombination line measurements.

5. CONCLUSION

Our results help us to infer the structure of the interstellar medium of M82. Using our models of the radio recombination line emission from the central starburst region, we can begin to understand how this starburst galaxy has evolved. This can lead to understanding how other similar galaxies are evolving. We can infer that the center region of M82 is composed of diffused gas at the lower frequencies. The outline of the data points in Figure 6 indicates there is some diffused gas at the lower frequency data points due to the enhancement of the recombination line emission. In order to produce a more realistic model, we must incorporate calculations for HII regions and synchrotron radiation to better understand the structure of M82. These models indicate there is a possible enhancement or stimulation of the emission. In the future, we hope to determine the relationship between the peak line emission and the continuum emission of the center region to further understand the recombination line emission at the lower frequencies.

6. ACKNOWLEDGEMENT

I would like to thank Dr. Kimberly Emig and the National Radio Astronomy Observatory for their help in conducting this research.

REFERENCES

Bell, M. B., & Seaquist, E. R. 1977, ApJ, 56, 461

Bell, M. B., Seaquist, E. R., Mebold, U., Reif, K., & Shaver, P. 1984, ApJ, 130, 1

Chaisson, E. J., & Rodriguez, L. F. 1977, ApJ, 214, L111

Puxley, P. J., Brand, P. W. J. L., Moore, T. J. T., et al. 1989, ApJ, 345, 163

Rodriguez-Rico, C. A., Viallefond, F., Zhao, J. H., Goss, W. M., & Anantharamaiah, K. R. 2004, ApJ, 616, 783

Seaquist, E. R., Carlstrom, J. E., Bignell, R. C., & Bell, M. B. 1985, ApJ, 294, 546
Seaquist, E. R., Carlstrom, J. E., Bryant, P. M., & Bell, M. B. 1996, ApJ, 465, 691
Seaquist, E. R., Kerton, C. R., & Bell, M. B. 1994, ApJ, 429, 612
Shaver, P. A., Churchwell, E., & Rots, A. H. 1977, ApJ, 55, 435